G Protein Activation by Serotonin Type 4 Receptor Dimers

EVIDENCE THAT TURNING ON TWO PROTOMERS IS MORE EFFICIENT[*][S]

Lucie P. Pellissier[‡§], Gaël Barthet[‡§], Florence Gaven[‡§], Elisabeth Cassier[‡§], Eric Trinquet[¶], Jean-Philippe Pin[‡§], Philippe Marin[‡§], Aline Dumuis[‡§], Joël Bockaert[‡§], Jean-Louis Banères[||], and Sylvie Claeysen[‡§1]

From the ‡Institut de Génomique Fonctionnelle, Université de Montpellier, CNRS UMR5203, F-34094 Montpellier, France, §INSERM, U661, F-34094 Montpellier, France, the ||Institut des Biomolécules Max Mousseron Faculté de Pharmacie, F-34093 Montpellier, France, and ¶CisBioInternational, F-30200 Bagnols sur Cèze, France

The discovery that class C G protein-coupled receptors (GPCRs) function as obligatory dimeric entities has generated major interest in GPCR oligomerization. Oligomerization now appears to be a common feature among all GPCR classes. However, the functional significance of this process remains unclear because, *in vitro*, some monomeric GPCRs, such as rhodopsin and β_2-adrenergic receptors, activate G proteins. By using wild type and mutant serotonin type 4 receptors (5-HT$_4$Rs) (including a 5-HT$_4$-RASSL) expressed in COS-7 cells as models of class A GPCRs, we show that activation of one protomer in a dimer was sufficient to stimulate G proteins. However, coupling efficiency was 2 times higher when both protomers were activated. Expression of combinations of 5-HT$_4$, in which both protomers were able to bind to agonists but only one could couple to G proteins, suggested that upon agonist occupancy, protomers did not independently couple to G proteins but rather that only one G protein was activated. Coupling of a single heterotrimeric G$_s$ protein to a receptor dimer was further confirmed *in vitro*, using the purified recombinant WT RASSL 5-HT$_4$R obligatory heterodimer. These results, together with previous findings, demonstrate that, differently from class C GPCR dimers, class A GPCR dimers have pleiotropic activation mechanisms.

G protein-coupled receptors (GPCRs)[2] are key players in cell-cell communication. They transduce a wide range of extracellular signals, such as light, odors, hormones, or neurotransmitters into appropriated cellular responses (1, 2). Signal transduction occurs via conformational changes of the ligand-activated GPCRs, leading to activation of G proteins and their downstream signaling pathways (3).

GPCRs have been considered for a long time as monomeric proteins, and the paradigm of "one ligand/one receptor/one G protein" was the driving principle (1). However, a growing number of studies revealed dimerization/oligomerization of GPCRs (4–8) mostly in heterologous cells (homo- or heterodimers) but also in native tissues or *in vivo* (dimers) (9–13). In line with these observations, a recent report described crystal structures of the chemokine receptor CXCR4 that are consistent with the formation of homodimers (14).

A relatively accepted model proposes that only one protomer in a dimer is fully activated, even when both binding sites are occupied (15–19). The activated protomer interacts with the Gα subunit to accelerate GDP/GTP exchange. This is compatible with recent data showing that a rhodopsin monomer (or a β_2-adrenergic receptor monomer) is sufficient to activate its cognate G protein after purification and reconstitution in a phospholipid bilayer (20, 21). However, some observations indicate that the active state of a GPCR dimer is asymmetric (22, 23) and that conformational switches occur between protomers (24, 25). Moreover, occupation of the second protomer of a dimer is probably not "silent" because it can either favor (26) or reduce (22) coupling efficiency. It has also been reported that occupation of both binding sites in 5-HT$_{2C}$ receptor dimers is mandatory for receptor activation (27).

Collectively, these reports suggest that the second protomer within GPCR homo- or heteromeric assemblies can be involved in different regulatory mechanisms. How such a diversity may be related to the physiological roles of the corresponding receptor and how it can influence signaling efficiency are poorly addressed questions.

Here, we analyzed the functional response elicited by different combinations of wild type (WT) and mutant 5-HT$_4$ receptor (5-HT$_4$R) dimers in a cellular context and *in vitro*, using purified proteins. These combinations allowed occupancy of one or both binding sites and the control of the coupling of each protomer to G proteins. We considered the receptor dimer·G protein entity as the minimal functional unit (28) because oligomeric entities can be viewed as multiples of dimers. Therefore, throughout we have used the term "dimer" to represent the minimal oligomeric arrangement.

We show that upon agonist occupation of both protomers, 5-HT$_4$R dimers were about twice as efficient in activating G proteins as following occupation of only one binding site. This may suggest that each protomer could be independently coupled to a G protein. However, we provide experimental evi-

---

[S] The on-line version of this article (available at http://www.jbc.org) contains supplemental Figs. 1–6.

[1] To whom correspondence should be addressed: Institut de Génomique Fonctionnelle, 141 Rue de la Cardonille, 34094 Montpellier Cedex 5, France. Tel.: 33-434-35-92-15; Fax: 33-467-54-24-32; E-mail: sylvie. claeysen@igf.cnrs.fr.

[2] The abbreviations used are: GPCR, G protein-coupled receptor; 5-HT, 5-hydroxytryptamine; 5-HT$_7$R and 5-HT$_4$R, serotonin receptor subtypes 7 and 4, respectively; GABA$_B$R, type B γ-aminobutyric acid receptor; mGluR, metabotropic glutamate receptor; mGlu$_7$R, metabotropic glutamate receptor subtype 7; PAC$_1$R, pituitary adenylate cyclase-activating polypeptide (PACAP) receptor subtype 1; IP1, inositol monophosphate; GTPγS, guanosine 5'-3-O-(thio)triphosphate.

dence suggesting that a single heterotrimeric G_s protein couples to a receptor dimer. These results were confirmed by *in vitro* experiments showing that activation of a single G_s protein was higher when both protomers within a dimer were occupied by an agonist.

EXPERIMENTAL PROCEDURES

Plasmid Constructs—Tagged-5-HT$_{4(a)}$R cDNA plasmids in pRK5 were generated by adding the c-Myc, HA, FLAG, or RhoTag epitopes to the N-terminal extremity of the receptor using the QuikChange site-directed mutagenesis kit (Stratagene, Amsterdam, The Netherlands) as described previously (29). Tagged 5-HT$_4$R-D100A (D100A), 5-HT$_4$R-D66N (D66N), 5-HT$_4$R-D66N/D100A (DD), 5-HT$_4$R-T104A (T104A), and 5-HT$_4$R-D330Stop (Δ329) mutants were generated from tagged 5-HT$_{4(a)}$R cloned in pRK5 using the same mutagenesis kit.

Antibodies—Rabbit anti-HA antibody (SG77) was purchased from Cliniscience (Montrouge, France). Rabbit anti-c-Myc antibody (A-14) was from Santa Cruz Biotechnology, Inc. (Santa Cruz, CA). Mouse anti-FLAG (M2) and mouse anti-c-Myc (9E10) antibodies were purchased from Sigma. Mouse anti-RhoTag antibody was provided by Dr. S. Costagliola (Institut de Recherche en Biologie Humaine et Nucléaire, Brussels, Belgium) (30). Alexa Fluor 488- and 594-labeled secondary antibodies were purchased from Invitrogen. Horseradish peroxidase-conjugated anti-rabbit and anti-mouse antibodies were from GE Healthcare.

Cell Cultures and Transfection—COS-7 cells were grown in Dulbecco's modified Eagle's medium (DMEM) supplemented with 10% dialyzed FCS and antibiotics. They were transfected at 60–70% confluence by electroporation as described previously (31) and processed for subsequent experiments.

Cell Surface ELISA—COS-7 cells in 96-well plates were transfected with WT and/or mutant tagged 5-HT$_4$R or GPCR plasmids. Twenty-four hours after transfection, cells were fixed with 4% (w/v) paraformaldehyde at room temperature for 5 min and blocked with phosphate-buffered saline containing 1% fetal calf serum (blocking buffer). Cells were then incubated with the appropriate antibody (anti-HA at 0.6 μg/ml, anti-Myc at 2.2 μg/ml, anti-FLAG at 4.4 μg/ml) in the same buffer for 60 min. After four washes with blocking buffer, cells were incubated with anti-rabbit (1 μg/ml) or anti-mouse/HRP conjugate (0.25 μg/ml) (GE Healthcare) for 60 min. After extensive washes, the chromogenic substrate was added (Supersignal® ELISA femto-maximum sensitivity; Pierce). Chemiluminescence was detected and quantified using a Wallac Victor2 luminescence counter.

Fluorescence Resonance Energy Transfer (FRET)—COS-7 cells were transfected with the appropriate plasmids and seeded in 96-well plates (100,000 cells/well). Twenty-four hours after transfection, cells were incubated with the appropriate fluorescent anti-FLAG, -HA, or -Myc antibodies diluted in 50 μl of HBS-KF (20 mM HEPES, 150 mM NaCl, 4.2 mM KCl, 0.9 mM CaCl$_2$, 0.5 mM MgCl$_2$, 0.1% glucose, 0.1% BSA, 200 mM KF) at 4 °C for 24 h. KF was added to avoid quenching of europium cryptate. Quantification of FRET signals was performed by homogeneous time-resolved fluorescence (HTRF®) using anti-

bodies coupled either to europium cryptate as a donor (Cisbio International, Bagnols-sur-Cèze, France) or to various acceptors (Alexa Fluor 647, Molecular Probes; d2, Cisbio International) (32).

Co-immunoprecipitation Experiments and Immunoblotting—COS-7 cells were seeded at 10^6/150-mm plate 48 h prior to the experiment and then transfected with RhoTag- or Myc-tagged WT and mutant 5-HT$_4$Rs as indicated in the figure legends. Cross-linking was carried out in phosphate-buffered saline (PBS) completed with 25 mM of dithiobis(succinimidyl propionate) (Pierce) for 30 min, as described previously (33). After 60 min of incubation at 4 °C, samples were processed as described (29), using a 1:1 mixture of Protein A/Protein G-Sepharose beads (GE Healthcare) that were precoupled with 8 μg of anti-Myc antibody (Polyclonal A-14, Santa Cruz Biotechnology, Inc.). Immunoprecipitated proteins were eluted in Laemmli sample buffer, resolved by SDS-PAGE, and detected by Western blotting.

Determination of cAMP or Inositol Monophosphate (IP1) Production in Transfected Cells—COS-7 cells were transfected with the appropriate plasmids and seeded in 24-well plates (100,000 cells/well for cAMP and 500,000 cells/well for IP1 measurements). Twenty-four hours after transfection, a 10-min (cAMP) or 30-min (IP1) stimulation with the appropriate concentrations of drugs was performed as described previously (29). cAMP or IP1 production was quantified by HTRF® using the cAMP Dynamic kit or the IP-One kit (Cisbio International, Bagnols-sur-Cèze, France), according to the manufacturer's instructions.

Membrane Preparation and Radioligand Binding Assay—Membranes were prepared from transiently transfected COS-7 cells plated in 15-cm dishes and grown in DMEM with 10% dialyzed FCS as described by Claeysen *et al.* (34). Membranes were homogenized in 50 mM HEPES (pH 7.4; 5 mg of proteins in 1 ml of solution) and stored at −80 °C until use. Membrane suspensions (about 10 μg), diluted in 100 μl of 50 mM HEPES containing 10 mM pargyline and 0.01% ascorbic acid, were incubated with 100 μl of [^{3}H]GR 113808 (specific activity, 82 Ci/mmol) and 50 μl of buffer or competing drugs at 20 °C for 30 min. For saturation analysis assays, various concentrations of [^{3}H]GR 113808 (0.001–0.8 nM) were used. BIMU8 (10 μM) was used to determine specific binding. To quantify [^{3}H]GR 113808 bound to WT receptors in cells co-expressing WT and D100A (or DD) 5-HT$_4$Rs, experiments were performed in the presence of 10 μM 5-HT, which does not bind to the D100A or DD mutants. The difference between the total [^{3}H]GR 113808 binding and the remaining binding measured in the presence of 5-HT corresponded to the [^{3}H]GR 113808 binding to co-expressed D100A (or DD) receptors. Protein concentration was determined by the bicinchoninic acidic method.

Data Analysis—The dose-response curves were fitted using GraphPad Prism and the following equation for monophasic dose-response curves: $y = (y_{max} - y_{min})/1 + ((x/EC_{50})\,n_H) + y_{min}$, where EC_{50} is the concentration of the compound needed to obtain 50% of the maximal effect, and n_H is the Hill coefficient. Competition and saturation experiments were evaluated by non-linear regression analysis using Prism. All represented data corresponded to the mean ± S.E. of three independent

experiments performed in triplicate. Statistical significance was determined with the Student-Newman-Keuls test using Prism.

Purified WT·D100A 5-HT$_4$R Dimer Preparation—5-HT$_4$R production and refolding were done as described (35). The WT·D100A dimer complex was obtained with a two-step purification process as already done for the BLT1 dimer (36). Briefly, S-tagged (WT) and Strep-tagged (D100A) 5-HT$_4$Rs were expressed as fusion proteins with KSI (the tag sequence was after the thrombin cleavage site). After removing KSI with thrombin (35), WT and D100A receptors were mixed, refolded, and purified as described (28). Refolded receptors were then immobilized on S-protein-agarose and eluted with 1 M MgCl$_2$. The protein fraction recovered under these conditions was then loaded onto a Streptactin affinity column (5.0 × 0.6 cm) and eluted with 2.5 mM dethiobiotin.

GTPγS-binding Assays—BODIPY FL GTPγS assays were carried out as described (37). Briefly, BODIPY-nucleotide binding to Gα$_s$ subunit was determined in 10 mM Hepes, 1 mM EDTA, and 10 mM MgCl$_2$, pH 8.0. Fluorescence measurements on a second to minute time scale were made in a 10-mm cell using a Cary Eclipse fluorimeter equipped with an RX.2000 rapid mixing stopped-flow unit (Applied Photophysics). In the association kinetics experiments, 1 μM ligand was added to 20 nM receptor and 200 nM Gα$_s$β$_1$γ$_2$ trimer, and then binding was initiated by the addition of the BODIPY-nucleotide. The change in fluorescence was measured over time and normalized to the base-line binding of the fluorescent BODIPY analog in the absence of agonist.

Fluorescence Measurements—IANBD (*N*-(iodoacetyl)-*N'*-(7-nitrobenz-2-oxa-1,3-diazol-4-yl)ethylenediamine) labeling of 5-HT$_4$R was carried out as described for the β_2-adrenegic receptor (38). Fluorescence emission spectra were recorded at 201C on a CaryEclipse spectrofluorimeter (Varian) with an excitation wavelength of 315 nm (bandwidth 2 nm). Receptor concentrations were in the 10^{-8} to 10^{-9} M range. Buffer contributions were subtracted under the same experimental conditions.

Chemical Cross-linking and Size Exclusion Chromatography—The stoichiometry of the receptor·G protein complex was assessed as described for the BLT1 receptor. Briefly, WT dimers, purified as described above and at a concentration of 10^{-6} M in the presence of the agonist (serotonin at an agonist/receptor molar ratio of 1:1), and trimeric Gα$_s$β1γ2 (receptor to G-protein molar ratio 1:10) were submitted to cross-linking for 5 h, at room temperature, after the addition of dTSP (125 mM stock solution in *N,N*-dimethylformamide) to a final concentration of 0.5 mM. The reaction was stopped by the addition of glycine to a final concentration of 50 mM. Cross-linked species were submitted to size exclusion chromatography, and the detergent was extracted as described (28). The resulting protein mixture was loaded onto a Superdex S200 HR column (10 × 300 mm; GE Healthcare). The chromatographic retention times were standardized using a gel filtration standard kit (Bio-Rad) comprising IgG (158 kDa), bovine serum albumin (66 kDa), ovalbumin (44 kDa), and myoglobin (17 kDa). The protein composition of each peak after elution was assessed by SDS-PAGE under reducing conditions (2-mercaptoethanol).

RESULTS

Pharmacological Properties of the 5-HT$_4$R Mutants Used in This Study—To study the functional role of the second protomer of 5-HT$_4$R dimers, we used different 5-HT$_4$-R mutants. The D100A mutant (supplemental Fig. 1) does not bind to 5-HT but can still be activated by synthetic molecules, such as the full agonist BIMU8 and also ML 10375, which acts as a full antagonist at WT 5-HT$_4$Rs (Fig. 1) (34). This mutant is one of the recently designed RASSLs (receptors activated solely by synthetic ligands) (34, 39). The D66N mutant poorly activates G$_s$ protein, does not display constitutive activity, and does not activate phospholipase C (PLC) (see Fig. 1 for cAMP data and Ref. 40 for cAMP and Ca^{2+}/inositol phosphate data). The DD double mutant (D100A/D66N mutation) does not bind to 5-HT and shows impaired G$_s$ protein-coupling. (Fig. 1) (40). The T104A mutant is activated by 5-HT and BIMU8 but not by benzamides, such as zacopride (Fig. 1) (41).
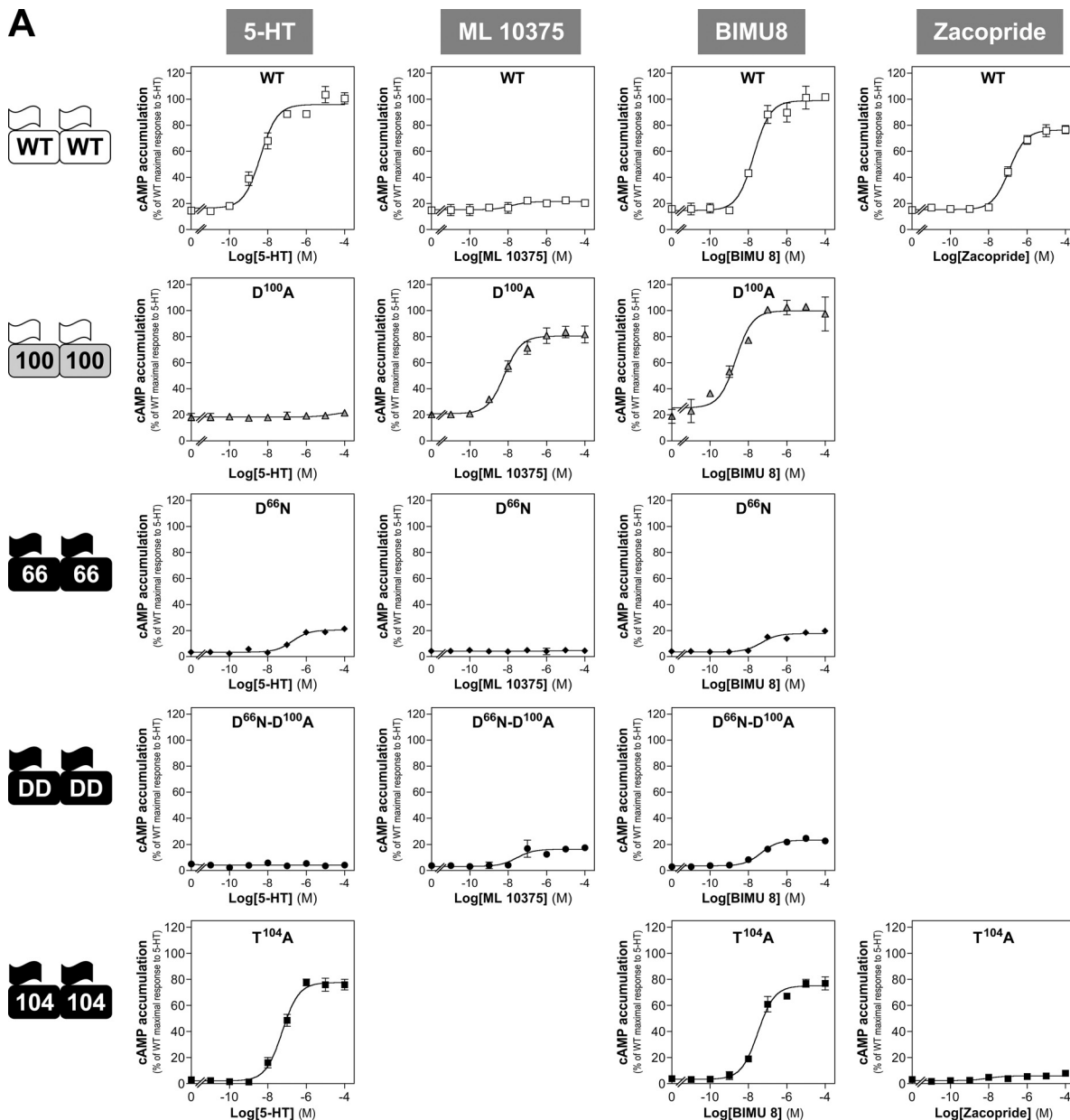
Dimerization of 5-HT$_4$R at the Cell Surface—Previous studies reported that 5-HT$_4$Rs form constitutive dimers in living cells (42). We used TR-FRET tools (32) to confirm that WT 5-HT$_4$R monomers could form homodimers and also heterodimers with mutant 5-HT$_4$Rs at the cell surface. To this aim, WT and mutant 5-HT$_4$Rs were tagged N-terminally with HA or FLAG epitopes and transiently co-transfected in COS-7 cells. As a positive control of constitutive dimerization, we used HA or FLAG-tagged GB$_1$ and GB$_2$ GABA$_B$ receptor subunits. Similar amounts of 5-HT$_4$Rs and GABA$_B$Rs were correctly expressed at the cell surface (Fig. 2*A*). However, the TR-FRET signal detected when HA- and FLAG-5-HT$_4$R were co-expressed (Fig. 2*B*) represented only 30% of the signal obtained for GABA$_B$R heterodimers. This difference might be explained by the fact that the GABA$_B$Rs expressed at the cell surface were obligatory heterodimers, whereas HA-5-HT$_4$R monomers could associate with either HA-5-HT$_4$R or FLAG-5-HT$_4$R. Hence, HA-5-HT$_4$R·FLAG-5-HT$_4$R dimers, which are the only couples producing FRET, represented only half of the real amount of dimers at the cell surface. One can thus assume that the real signal for 5-HT$_4$R dimers was around 60% of the GABA$_B$R FRET signal. Similarly, all of the 5-HT$_4$R mutants were correctly expressed at the cell surface (Fig. 2*E*) and produced FRET signals comparable with those of WT 5-HT$_4$R dimers (Fig. 2*F*). Formation of 5-HT$_4$R homo- or heterodimers was further confirmed by co-immunoprecipitation (supplemental Fig. 2).

We then maintained a constant density of HA-5-HT$_4$Rs (donors) and increased the density of FLAG-5-HT$_4$R or FLAG-GB$_2$ (acceptors). Using WT or DD 5-HT$_4$Rs, we obtained saturating FRET curves, whereas the signal between 5-HT$_4$R and GB$_2$ remained linear and unsaturable (Fig. 2*C*). These results indicate that 5-HT$_4$R homodimerization was specific, whereas the 5-HT$_4$R·GB$_2$ signal reflected a collisional and nonspecific contact as suggested also by their FRET emission that corresponded to only 8% of the signal for GABA$_B$R heterodimers (Fig. 2*A*).

To further investigate the specificity of 5-HT$_4$R homodimerization, we performed competition experiments. Constant amounts of HA- and FLAG-5-HT$_4$R were co-expressed with increasing amounts of competing GPCRs belonging to different

A

Figure panel A: Dose-response curves of cAMP accumulation (% of WT maximal response to 5-HT) versus Log concentration (M) for four ligands (5-HT, ML 10375, BIMU8, Zacopride) across five receptor dimer constructs (WT/WT, 100/100, 66/66, DD/DD, 104/104), showing labeled plots: WT, D¹⁰⁰A, D⁶⁶N, D⁶⁶N-D¹⁰⁰A, T¹⁰⁴A.

B

	5-HT	ML 10375	BIMU 8	Zacopride
WT	$4.2 \pm 1.4 \times 10^{-9}$	ND	$1.9 \pm 0.8 \times 10^{-8}$	$1.2 \pm 1.1 \times 10^{-7}$
D100A	ND	$6.4 \pm 1.2 \times 10^{-9}$	$2.2 \pm 1.0 \times 10^{-9}$	
D66N	$1.9 \pm 1.4 \times 10^{-8}$	ND	$4.7 \pm 1.8 \times 10^{-8}$	
D66N-D100A (DD)	ND	$2.8 \pm 2.2 \times 10^{-8}$	$4.5 \pm 1.2 \times 10^{-8}$	
T104A	$5.5 \pm 1.2 \times 10^{-8}$		$3.1 \pm 1.2 \times 10^{-8}$	ND

C

Figure panel C: Three plots versus WT cDNA (ng): Expression (Cell surface expression, ELISA arbitrary units and Receptor density, pmol/mg of protein; ELISA open squares, Binding filled squares), cAMP (cAMP accumulation, pmol/100 000 cells; 5-HT), and IP1 (IP1 accumulation, pmol/100 000 cells; 5-HT).

classes: class A (5-HT$_7$R and thyroid-stimulating hormone receptor), class B (PAC$_1$R), and class C (mGluR$_7$ and GABA$_{B2}$R). GABA$_{B2}$R (GB$_2$) was unable to compete with 5-HT$_4$R homodimerization (Fig. 2D). Thyroid-stimulating hormone receptor, mGluR$_7$, PAC$_1$R, and 5-HT$_7$R competed with the formation of 5-HT$_4$R homodimers to different extents but only at high and probably not physiological concentrations. By contrast, Myc-5-HT$_4$R potently reduced the FRET signal and competed with HA- and FLAG-5-HT$_4$R for dimer formation.

Agonist Occupation of Two 5-HT$_4$R Protomers Activates the G$_s$ Signaling Pathway More Efficiently than Occupation of a Single Protomer—We first verified that the densities of the expressed receptors (assessed by ELISA and radioligand binding assays; see Fig. 1C for WT 5-HT$_4$R) were proportional to the quantity of transfected cDNA (up to 250 ng/10^7 cells). The magnitude of second messenger accumulation (cAMP or IP1) was also proportional to the receptors' densities, a prerequisite to compare the responses obtained with different dimers (Fig. 1C).

To assess whether both protomers of 5-HT$_4$R dimers needed to be activated to induce the G$_s$ signaling pathway, we transfected COS-7 cells with WT 5-HT$_4$R and/or the double mutant (DD) that does not bind to 5-HT and does not induce cAMP production (Figs. 1A and 3A). Exposure to 5-HT of cells transfected with the DD mutant alone did not induce cAMP production (Fig. 3B). Conversely, exposure to 5-HT of cells that expressed WT 5-HT$_4$R alone or in combination with DD 5-HT$_4$R provided overlapping dose-response curves (Fig. 3, A and B). Similar densities of WT or DD 5-HT$_4$Rs were measured in cells expressing WT or DD 5-HT$_4$R alone (4.3 ± 0.7 and 4.9 ± 1.0 pmol/mg protein, respectively) and in cells that coexpressed the two protomers (4.5 ± 0.6 and 5.6 ± 0.8 pmol/mg protein, respectively). Therefore, the total receptor density was 2 times higher in co-transfected cells than in cells transfected with either WT or DD 5-HT$_4$R. Hence, if we arbitrarily set the dimer density in co-transfected cells at 4d, the density in cells transfected with either WT or DD 5-HT$_4$R will be 2d (Fig. 3C). Specifically, in co-transfected cells, three dimer species are theoretically formed (WT·WT, WT·DD, and DD·DD) and their respective densities will be d, 2d, and d (Fig. 3, A and C). If the occupation of one protomer by 5-HT is sufficient to fully activate dimers, WT·WT and WT·DD dimers would be similarly activated by 5-HT, and the total activation would be more elevated in co-transfected cells than in cells expressing WT 5-HT$_4$R alone (H1 hypothesis; Fig. 3C). This differed from what we observed experimentally. We therefore reasoned that WT·DD dimers, in which only one protomer is activated by 5-HT, are able to generate cAMP but less efficiently (about 2 times less) than WT·WT homodimers (H2 hypothesis; Fig. 3C). In this hypothesis, the 5-HT dose-response curves in cells

FIGURE 2. **5-HT$_4$ receptors form specific homodimers at the cell surface.** *A*, COS-7 cells were transiently transfected with plasmids encoding epitope-tagged 5-HT$_4$R (250 ng/10^7 cells) and/or GABA$_B$R (1,000 ng/10^7 cells). Cell surface expression of 5-HT$_4$R and GABA$_B$R expressed alone or in combination was assessed by ELISA using anti-HA (in *white*) or anti-FLAG (in *black*) antibodies in non-permeabilized, transfected cells. *GB$_1$*, GABA$_{B1}$R; *GB$_2$*, GABA$_{B2}$R. *B*, TR-FRET between donor and acceptor fluorophore-labeled antibodies directed against the HA and FLAG tags, respectively, placed at the N terminus of 5-HT$_4$R and GABA$_B$R as exemplified *below* the graph. Tagged GABA$_B$ receptor subunits GB$_1$ and GB$_2$ were used as a positive control of constitutive dimerization. *C*, saturation FRET experiments. A constant amount of WT HA-5-HT$_4$R (donor) was co-expressed with increasing amounts of FLAG-tagged 5-HT$_4$R-D66N (*DD*), WT 5-HT$_4$R, or GB$_2$ (acceptor). The FRET signal was plotted as a function of cell surface expression of the FLAG-tagged receptors determined by ELISA. *D*, competition FRET experiments. A constant amount of WT HA-5-HT$_4$R and FLAG-5-HT$_4$R was expressed, and the FRET corresponding to their association was determined in the presence of increasing amounts of Myc-tagged GPCRs belonging to different classes. The FRET signal was plotted as a function of cell surface expression of the Myc-tagged receptors determined by ELISA. Challenger GPCRs were as follows: 5-HT$_7$R and 5-HT$_4$R and thyroid-stimulating hormone receptor (*TSHR*) (class A); PAC$_1$R (class B); and mGlu$_7$R and GABA$_{B2}$R (GB$_2$) (subunit of the GABA$_B$ receptor that reaches the cell surface alone) (class C). *E*, cell surface expression of co-transfected WT and mutant 5-HT$_4$Rs. ELISA was performed using anti-HA (in *white*) or anti-FLAG (in *black*) antibodies in non-permeabilized cells expressing the different HA- or FLAG-tagged receptors. *F*, TR-FRET between donor and acceptor fluorophore-labeled antibodies directed against the HA and FLAG tags, respectively, placed at the extracellular N terminus of WT and mutant 5-HT$_4$Rs. *Error bars*, S.E.

FIGURE 1. **Pharmacological characteristics of the WT and mutant 5-HT$_4$ receptors and non-saturable second messenger accumulation under the experimental conditions used in the study.** *A*, cAMP accumulation. Schematic representations of the different receptor homodimers are presented on the *left*: WT 5-HT$_4$R (*WT*), D100A mutant (*100*), D66N mutant (*66*), D66N/D100A double mutant (*DD*), and T104A mutant (*104*). The graphs show cAMP accumulation induced by stimulation of the different receptors (50 ng of cDNA) with increasing concentrations of 5-HT, ML 10375, BIMU8, or zacopride. Each value was expressed as the percentage of the cAMP production (5.1 ± 0.2 pmol/100,000 cells) induced by 10^{-5} M 5-HT in cells expressing WT 5-HT$_4$R. *B*, EC$_{50}$ values of the experiments described in *A*. Results are means ± S.E. of the values obtained in three independent experiments performed with different sets of cultured cells. *C*, receptor density (ELISA and binding) data, cAMP accumulation, and IP1 production of WT 5-HT$_4$R were plotted as a function of the amount of transfected cDNA/10^7 cells. *Error bars*, S.E.
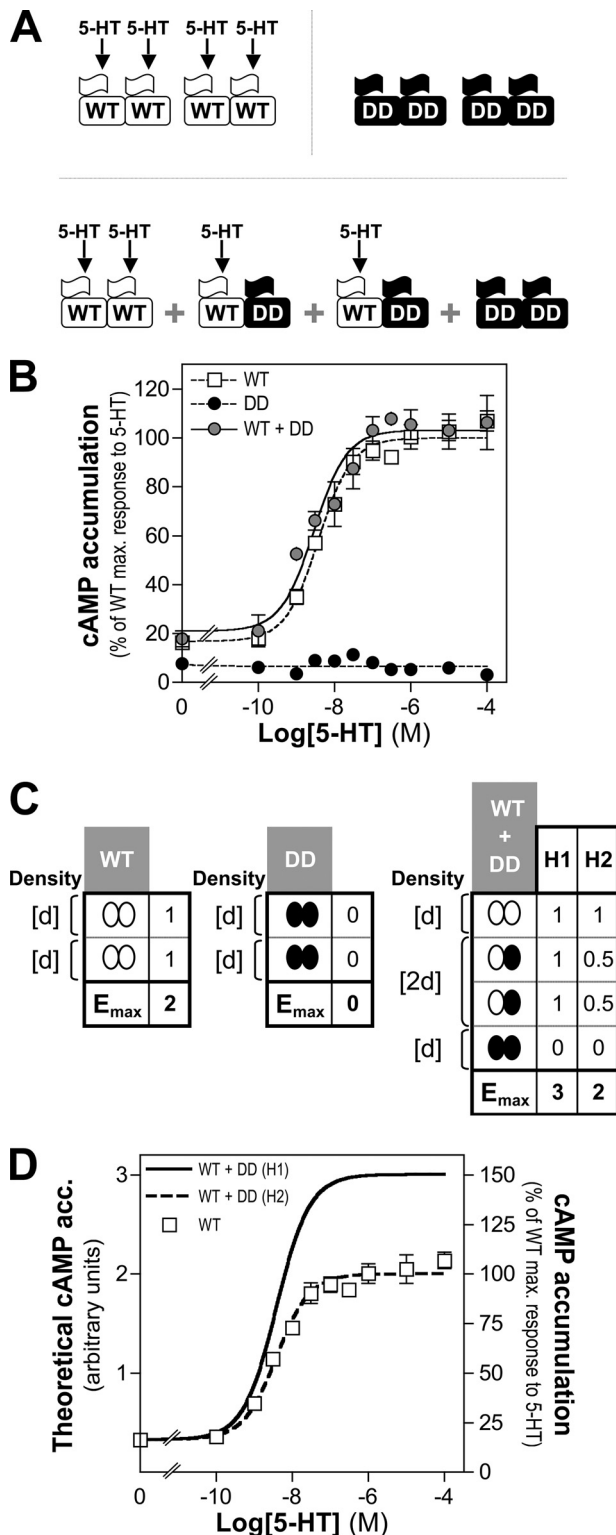
FIGURE 3. **Agonist occupancy of two 5-HT$_4$R protomers activates G$_s$ signaling more efficiently than occupancy of a single protomer.** COS-7 cells were transiently transfected with plasmids encoding WT and D66N/D100A (DD) 5-HT$_4$Rs (50 ng) alone or in association. *A*, schematic representation of the theoretical dimer populations. 5-HT activates the WT protomer but not the DD mutant. *B*, cAMP accumulation following 5-HT stimulation of cells that express WT or/and DD receptors. Each value was expressed as the percentage of the cAMP production (5.1 ± 0.2 pmol/100,000 cells) induced by 10^{-5} M 5-HT in cells expressing WT 5-HT$_4$R. *C*, theoretical maximal activity (*E*$_{max}$) reached by the different dimer populations according to the H1 and H2 hypotheses (see "Results" for full development of the reasoning). *Open ovals,*
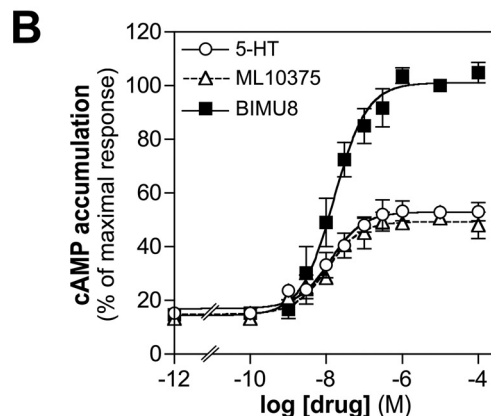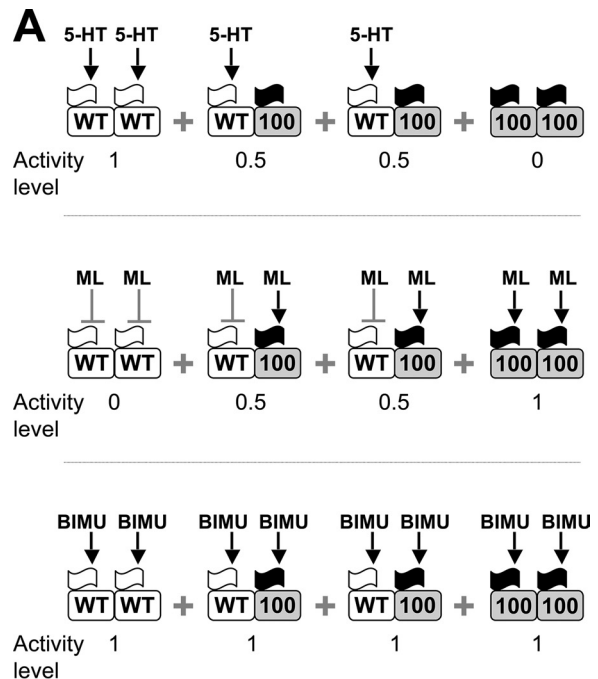

FIGURE 4. **Comparison between the cAMP productions induced by occupancy of one or two protomers within the same dimer population.** *A*, theoretical dimer populations expected upon expression in COS-7 cells of WT and D100A (*100*) 5-HT$_4$Rs at equivalent densities (4.1 ± 0.6 and 4.8 ± 0.9 pmol/mg protein, respectively). 5-HT only activates WT protomers. ML 10375 (*ML*) is an antagonist at WT receptors and an agonist at D100A receptors. BIMU8 (*BIMU*) activates both WT and D100A protomers. *B*, cAMP accumulation induced by stimulating cells with 5-HT, ML 10375, or BIMU8. Each value was expressed as the percentage of the cAMP production (9.9 ± 0.3 pmol/ 100,000 cells) induced by BIMU8 (10^{-5} M). *Error bars*, S.E.

expressing WT 5-HT$_4$R alone or in combination with DD 5-HT$_4$R should be comparable, which corresponds to experimental results (Fig. 3*D*). Further supporting this hypothesis, the D66N·D100A heterodimer occupied by ML 10375, which activates the D100A protomer but not the D66N protomer, was 50% less active than the D100A·D100A dimer in which both protomers were occupied by ML 10375 ([supplemental Fig. 3](#)).

WT promoters; *black ovals*, DD protomers. Their corresponding density (*d*) is indicated on the *left* of the *tables*. *D*, comparison between the experimental cAMP accumulation measured upon stimulation of WT receptors alone (2*d*) and the theoretical cAMP accumulation resulting from stimulation of co-expressed WT (2*d*) and DD (2*d*) receptors according to the H1 and H2 hypotheses. *Error bars*, S.E.
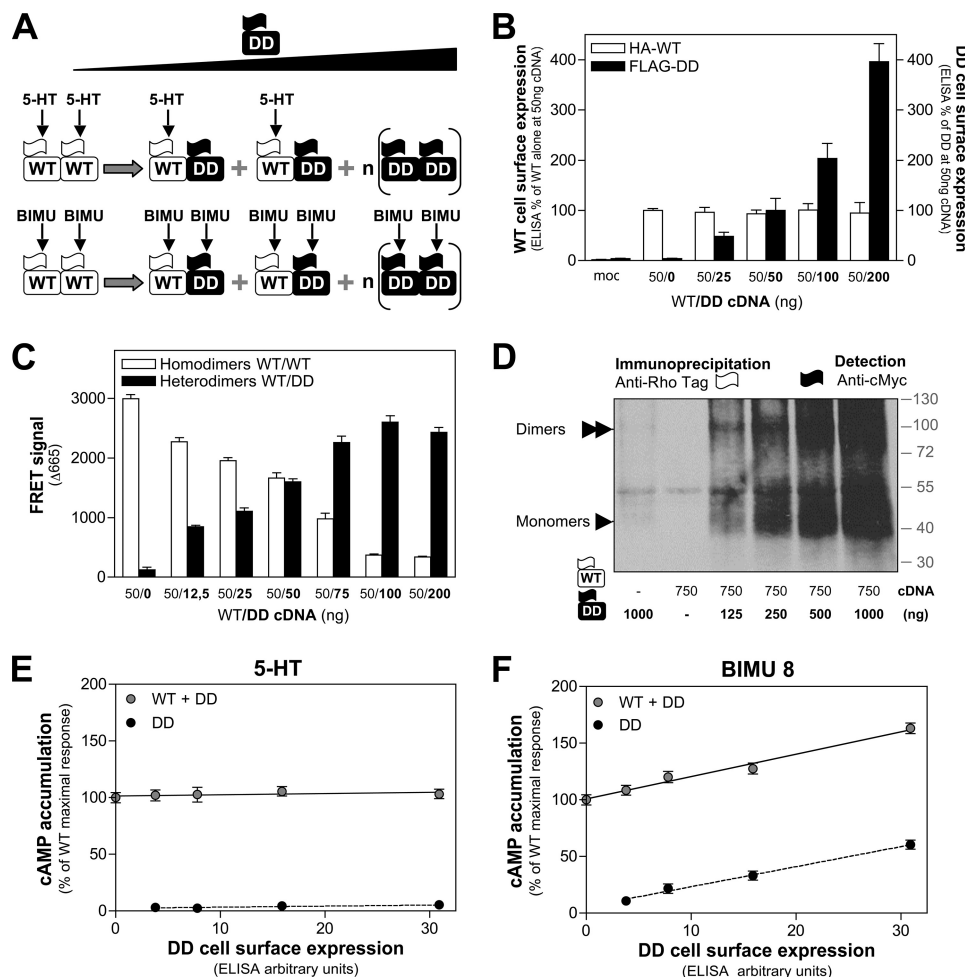
FIGURE 5. **Functional responses of cells in which the WT 5-HT$_4$R protomer was co-transfected with increasing concentrations of a non-responding protomer.** *A*, theoretical dimer populations in cells co-transfected with a constant amount of WT HA-5-HT$_4$R (*WT*) plasmid (50 ng of cDNA/10[7] cells) and increasing amounts of FLAG-D66N/D100A (DD) 5-HT$_4$R plasmid. 5-HT activates only WT protomers, whereas BIMU8 (*BIMU*) activates both WT and DD. *B*, cell surface expression of WT and DD receptors. ELISA was performed using anti-HA (in *white*) or anti-FLAG (in *black*) antibodies in non-permeabilized cells expressing the different receptors, each carrying an N-terminal HA or a FLAG tag. Values *below* the graph indicate the amount (in ng) of co-transfected cDNA plasmids (WT·DD). WT 5-HT$_4$R densities were 4.3 ± 0.7, 4.1 ± 0.8, 4.5 ± 0.6, 4.3 ± 0.9, and 4.1 ± 1.0 pmol/mg protein in cells transfected with WT/DD cDNA ratios of 50:0, 50:25, 50:50, 50:100, and 50:200, respectively. DD 5-HT$_4$R densities were 2.2 ± 0.3, 5.6 ± 0.8, 7.8 ± 1.1, and 15.4 ± 1.7 pmol/mg protein in cells transfected with 25, 50, 100, and 200 ng of DD cDNA, respectively. *C*, TR-FRET between WT 5-HT$_4$R and DD double mutant that were N-terminally tagged with the HA and FLAG epitopes, using donor and acceptor fluorophore-labeled antibodies directed against the tags. *White bars* indicate FRET signal between HA-WT and FLAG-WT expressed in a constant amount (25 ng of each construct) and HA-WT co-expressed with increasing amounts of Myc-DD double mutant. In an experiment performed in parallel, *black bars* indicate FRET signal between HA-WT (50 ng of cDNA) co-expressed with increasing amounts of FLAG-DD double mutant. Values *below* the graph indicate the amount of co-transfected cDNA (WT·DD) in ng. *D*, co-immunoprecipitation of increasing amounts of Myc-DD 5-HT$_4$R with a constant amount of RhoTag-WT receptor. Immunoprecipitation was performed using anti-RhoTag antibodies, and the blot was revealed using anti-c-Myc antibodies. Values *below* the image indicate the amounts of co-transfected cDNAs in ng. *E* and *F*, cAMP accumulation following stimulation with 5-HT (*E*) or BIMU8 (*F*). Each value was expressed as a percentage of the cAMP production (5.5 ± 0.2 pmol/100,000 cells) induced by 5-HT (10^{-5} M) in cells expressing only the WT receptor (*E*) or as a percentage of the cAMP production (5.7 ± 0.3 pmol/100,000 cells) induced by BIMU8 (10^{-5} M) in cells expressing only the WT receptor (*F*). *Error bars*, S.E.

Then, to compare the maximal cAMP level obtained by activating one or two protomers in the same dimer population, COS-7 cells, in which WT and D100A 5-HT$_4$Rs were co-expressed at equivalent densities (4.1 ± 0.6 and 4.8 ± 0.9 pmol/mg protein, respectively), were incubated with 5-HT, ML 10375, or BIMU8 (5-HT activates only the WT protomer, ML 10375 only the D100A protomer, and BIMU8 both protomers; Fig. 4*A*). The maximal cAMP level measured upon BIMU8 stimulation (normalized to 100%) was about twice the level obtained following incubation with 5-HT or ML 10375 (52.9 ± 1.1 and $49.4 \pm 1.3\%$ of the BIMU8 maximal response, respectively; Fig. 4*B*). This is consistent with our hypothesis that turning on one protomer within a dimer produces about half of the activity obtained by activating both protomers.

We next modified the equilibrium between 5-HT$_4$R dimers by progressively increasing the number of non-responding protomers (DD) while the amount of responding protomers (WT) was kept constant (Fig. 5, *A* and *B*). This resulted in a decrease in WT·WT dimers and a concomitant increment in WT·DD dimers, as indicated by TR-FRET (Fig. 5*C*) and co-immunoprecipitation experiments (Fig. 5*D*). However, 5-HT-induced cAMP production remained constant, whatever the amount of DD mutant expressed (Fig. 5*E*), further supporting our hypothesis that WT·DD heterodimers are less active than WT·WT homodimers (see supplemental Fig. 4 for theoretical results). As expected, cAMP production upon exposure to BIMU8, which activates both WT and DD protomers, increased concomitantly with DD expression, indicating that
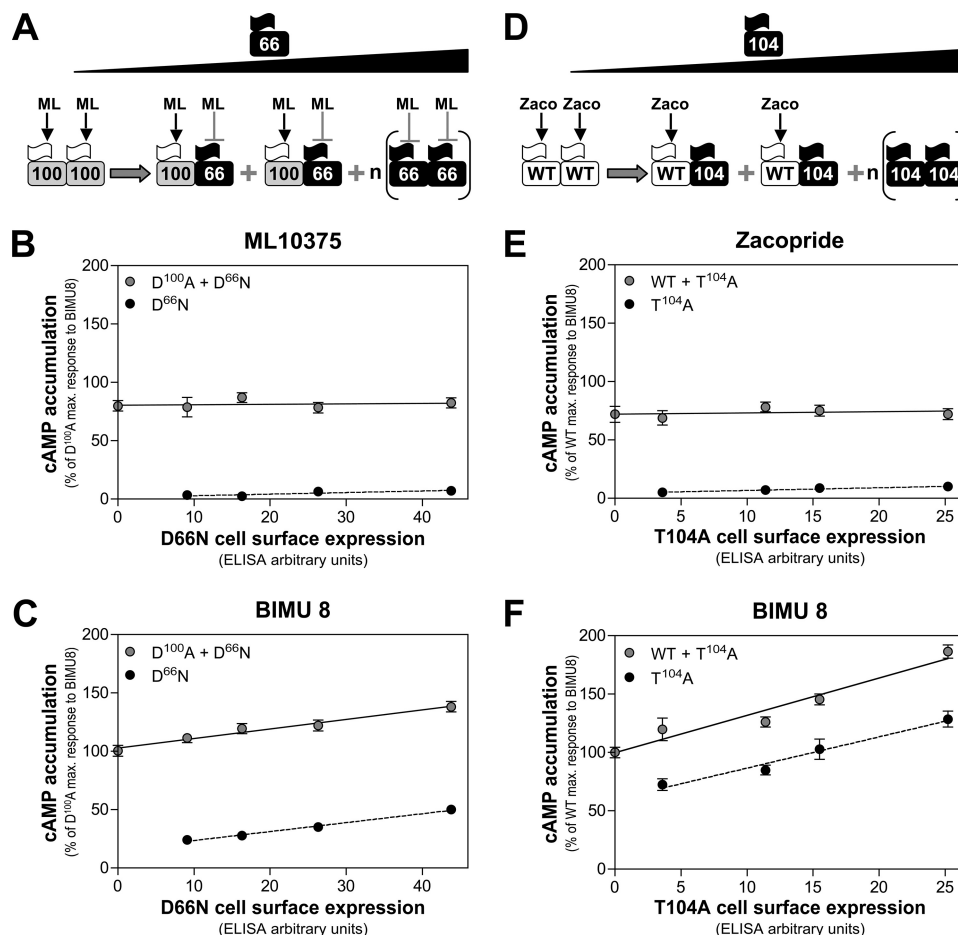
FIGURE 6. **Functional responses induced by dimers obtained by transfection of a constant amount of responding protomers and increasing concentrations of non-responding protomers.** *A* and *D*, theoretical dimer populations in cells co-transfected with a constant amount (50 ng) of D100A (*100*) 5-HT$_4$R plasmid and increasing amounts of D66N (*66*) 5-HT$_4$R plasmid (*A*) and in cells co-transfected with a constant amount (50 ng) of WT 5-HT$_4$R (*WT*) plasmid and increasing amounts of T104A (*104*) 5-HT$_4$R plasmid (*D*). ML 10375 (*ML*) acts as an agonist at the D100A protomer and as an antagonist at the D66N mutant. Zacopride (*Zaco*) activates WT but not T104A protomers. *B, C, E,* and *F*, cAMP accumulation following stimulation (each at 10^{-5} M) of the co-expressed receptors with ML 10375 (*B*), zacopride (*E*), or BIMU8 (*C* and *F*). Each value was expressed as a percentage of the cAMP production (6.4 ± 0.4 pmol/100,000 cells) induced by BIMU8 in cells expressing D100A 5-HT$_4$R (*B* and *C*) or as a percentage of the cAMP production (6.1 ± 0.3 pmol/100,000 cells) induced by BIMU8 in the cells expressing WT 5-HT$_4$R (*E* and *F*). *Error bars*, S.E.

the cAMP detection system was not saturated (Fig. 5*F*). Similarly, an increase in cAMP production was observed following expression of increasing amounts of WT 5-HT$_4$R ([supplemental Fig. 5](#)). To ensure that these observations were independent of the mutants and the drugs used, we investigated the functional response generated by different dimer couples. Activation of only the D100A protomer by ML 10375 (34) in D66N·D100A dimers or induction of only the WT protomer by zacopride (41) in WT·T104A dimers did not change the production of cAMP in COS-7 cells in which constant amounts of D100A or WT 5-HT$_4$Rs were co-transfected with increasing concentrations of D66N or T104A 5-HT$_4$Rs (Fig. 6).

Protomers of 5-HT$_4$R Dimers Do Not Independently Couple to G Proteins—Our results suggest that agonist-induced activation of both protomers of 5-HT$_4$R dimers induces a 2-fold greater activation of cAMP production than occupation of one protomer. We next explored whether simultaneous occupation of the two protomers conferred to 5-HT$_4$R dimers a structure able to activate more efficiently a single G protein than occupation of a single protomer or whether each occupied protomer independently activated its own G protein.

To discriminate between these two possibilities, we needed a dimer combination in which a fully active protomer (D100A) was associated with a protomer that could bind to a ligand, and thus adopt an "active" conformation, but was "completely inactive" for coupling to G protein (Fig. 7*A*). Because a protomer that does not activate the G$_s$-cAMP pathway was not available, we took advantage of the capacity of 5-HT$_4$Rs to activate PLC in COS-7 cells. D66N 5-HT$_4$R binds to all agonists, including BIMU8 (40), but it did not induce inositol monophosphate (IP1) production upon activation by BIMU8 (Fig. 7*B*). When BIMU8 was used as an agonist, the D66N·D100A dimer exhibited a level of activity comparable with that of a dimer (D100A·D100A) in which both protomers can activate the PLC effector pathway (Fig. 7*B*). This ruled out the hypothesis that each protomer activates its own G protein.

Conformational Switch between Protomers and Faster Activation of G$_s$ Proteins upon Occupation of both Protomers—To further confirm these observations *in vitro*, we produced a recombinant WT·D100A 5-HT$_4$R dimer stabilized in detergent solution, as previously described for the BLT1 receptor (35, 36) (see Fig. 8*A* for the purification steps). Ligand binding experi-
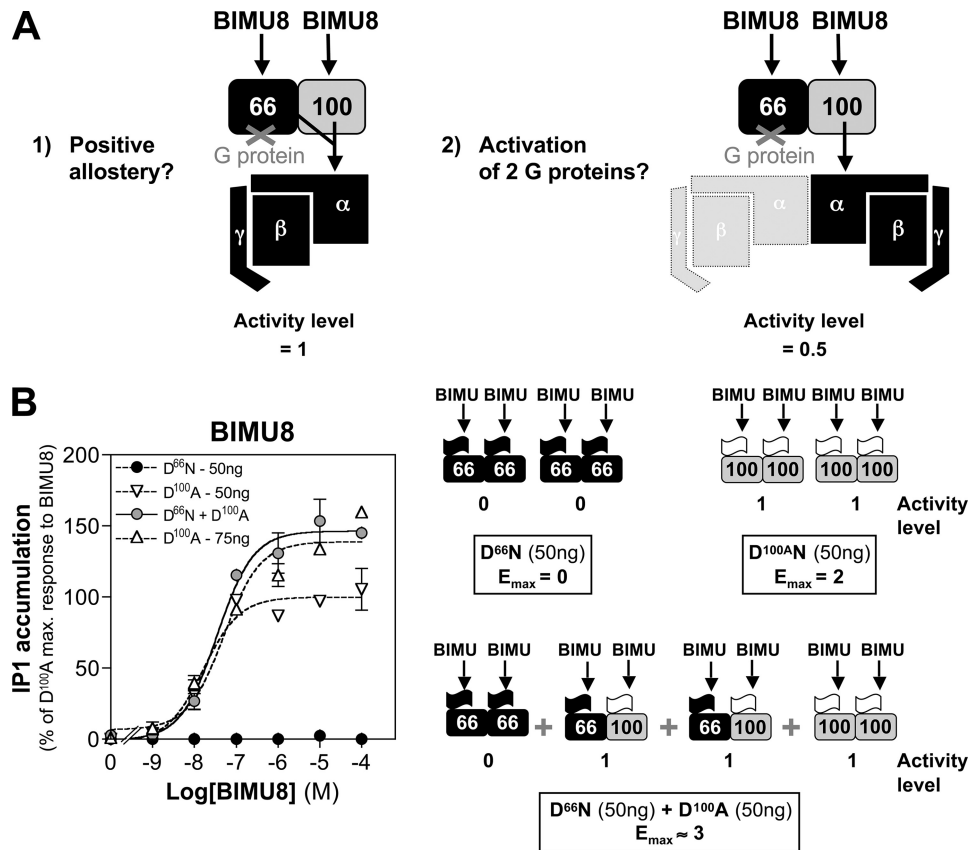
FIGURE 7. **A single G protein is similarly activated by a dimer composed of a "G-protein coupling-deficient" protomer and a fully functional protomer or by a dimer composed of two fully functional protomers.** *A*, theoretical receptor·G protein complexes according to the two hypotheses: the D66N·D100A heterodimer is either coupled to one heterotrimeric G protein (hypothesis 1) or to two heterotrimeric G proteins (hypothesis 2). BIMU8 can bind to both protomers and induces the stabilization of their "active" state. The D100A protomer is coupled to G_q and can induce IP1 production (*B*), whereas the D66N mutant cannot activate the Gq-PLC pathway. In hypothesis 1, an allosteric positive conformational switch between protomers results in full activation of one single G protein. BIMU8 stabilizes the "active" state of both protomers (even if the functional coupling of the D66N is dead) and induces an activity level of 1, in terms of IP1 production. In hypothesis 2, each protomer is coupled independently to one G protein. Because one protomer (D66N) is deficient in G protein activation, BIMU8 induces an activity level of 0.5, in terms of IP1 production. *B*, BIMU8-induced IP1 accumulation in cells expressing D66N and/or D100A 5-HT₄R. Densities of D66N and D100A receptors were 5.1 ± 0.8 and 4.6 ± 0.5 pmol/mg protein in cells transfected with 50 ng of cDNA of each receptor alone. Densities were 4.7 ± 1.1 for D66N and 4.2 ± 0.8 pmol/mg for D100A in co-transfected cells (50 ng of each cDNA). D100A 5-HT₄R density was 6.4 ± 0.5 pmol/mg in cells transfected with 75 ng of D100A 5-HT₄R cDNA alone. IP1 values were expressed as the percentage of the IP1 production (8.9 ± 0.5 pmol/100,000 cells) induced by BIMU8 (10^{-5} M) in cells transfected only with 50 ng of D100A plasmid. *Error bars*, S.E.

ments to evaluate the formation of WT·D100A dimers indicated that 5-HT displaced only half of the tritiated antagonist GR 113808 bound to the purified dimeric complex (Fig. 8*B*). The stoichiometry of the 5-HT₄R dimer·G_s protein assembly was investigated by chemical cross-linking followed by size exclusion chromatography (28). A major species was observed with a chromatographic mobility compatible with that of a complex resulting from the association of a single heterotrimeric G_s protein with a receptor dimer (Fig. 9*A*). Indeed, the calculated mass for such a complex (181,926 Da) corresponded to the experimental value estimated from the chromatographic mobility of the molecular weight standards (Fig. 9*A*).

To monitor receptor activation, we mutated all of the dye-accessible cysteines of WT or D100A protomers into serine residues except for cysteine 262, which is located at the cytoplasmic end of TM6 in both protomers (see supplemental Fig. 1 for Cys[262] location). This residue was labeled with the environment-sensitive dye IANBD to selectively monitor ligand-induced changes in the conformation of the modified protomer (38). This modification did not alter their binding properties and functional status (data not shown). As demonstrated for

the BLT1 receptor (36), two conformational changes were observed upon agonist activation of one protomer. The conformational change of the unliganded protomer of the dimer was smaller than the change of the agonist-liganded protomer. However, a clear conformational switch between protomers within the dimer was detected upon agonist occupation of only one protomer (Fig. 8*C*).

We then analyzed GTPγS binding to Gα_S induced by activation of one or two protomers in purified WT·D100A dimers. The initial rate of WT·D100A-catalyzed GTPγS binding to G proteins was faster in the presence of BIMU8, which activates both protomers, than in the presence of 5-HT or ML 10375, which activate only one protomer, (WT and D100A, respectively; Fig. 9*B*). The kinetic constants for receptor-catalyzed GTPγS binding to Gα_s were 0.18 ± 0.01 min^{-1} (with 5-HT), 0.17 ± 0.02 min^{-1} (with ML 10375), and 0.25 ± 0.02 min^{-1} (with BIMU8), confirming that the G_s protein was activated more efficiently when both protomers were turned on.

Asymmetric Positioning of the G_s Protein upon Receptor Activation—To explore how the α subunit of G_s protein (Gα_s) interacts with each protomer in a dimer, we performed FRET
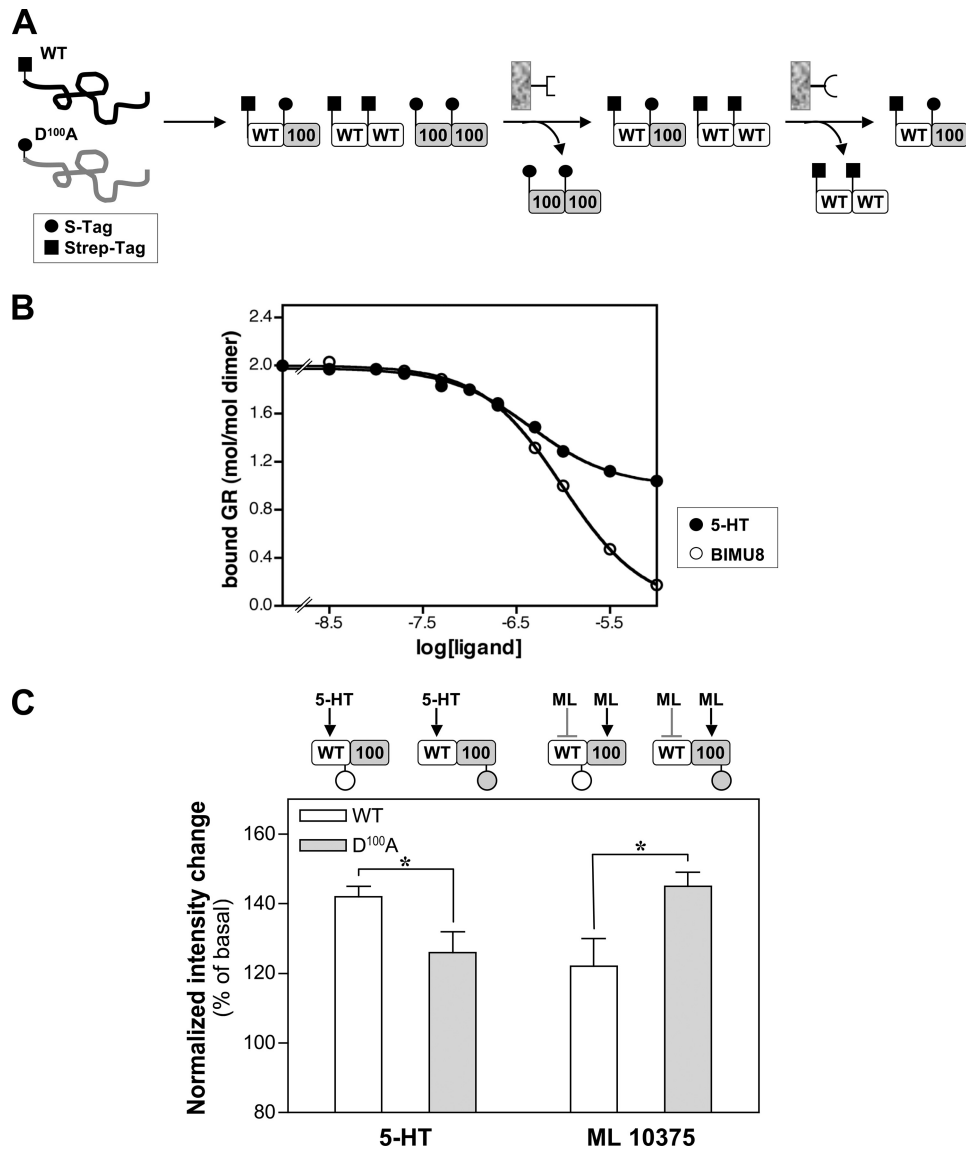
FIGURE 8. **Production and activation of purified WT·D100A 5-HT$_4$R dimers in solution.** *A*, schematic representation of the two-step procedure used to obtain purified WT·D100A 5-HT$_4$R dimers. *WT*, WT 5-HT$_4$R; *100*, D100A protomer. *B*, [^{3}H]GR 113808 binding to WT·D100A 5-HT$_4$R dimers and its displacement by 5-HT (*closed circles*) or by BIMU8 (*open circles*). 5-HT displaced only half of bound [^{3}H]GR 113808. Binding data are represented as a plot of the binding degree *x* as a function of the ligand concentration. The binding degree is defined by the mol of bound ligand/mol of receptor ratio. The experiments illustrated are representative of three independent trials, each performed in duplicate. *C*, relative change in NBD fluorescence in the presence of 5-HT or ML 10375 (*ML*) in WT·D100A dimers where one or the other of the protomers is labeled. A schematic representation of the dimer populations (*open boxes*: WT protomers; *gray boxes*, D100A protomers; *circles*, labeling dye) is depicted *above* the graph. Data are the means ± S.D. (*error bars*) of values calculated from three independent experiments. *, $p < 0.05$ *versus* the corresponding value obtained by changing the labeled protomer (Student's *t* test).

experiments in which the WT or D100A protomers of purified WT·D100A dimers were labeled with the fluorescence donor (Alexa Fluor 468) at cysteine 262 (see above), and Gα_s was labeled at its N terminus with the acceptor (Alexa Fluor 568; see "Experimental Procedures"). This modification did not affect Gα_s functionality, as shown by the similar receptor-catalyzed GDP/GTP exchange rates at unmodified and modified Gα_s proteins (0.26 and 0.23 min^{-1}, respectively).

When the WT subunit was labeled with the fluorescence donor, challenging with 5-HT (which activates only the WT protomer) produced a much lower FRET signal than following challenge with ML 10375 (which induces the D100A protomer) (Fig. 10*A*). This indicates that the labeled N terminus of Gα_s was near the labeled WT protomer when ML 10375 was bound

to the dimer and that it was in the inverse orientation (*i.e.* the N-terminal part of Gα_s was close to the D100A protomer) following challenge with 5-HT (Fig. 10*B*). In other words, the C terminus of Gα_s was close to the activated protomer, consistent with previous reports (43, 44). Moreover, the FRET signal induced by BIMU8, which binds to both protomers, was about half of the signal observed following ML 10375 stimulation and about twice the 5-HT-induced signal (Fig. 10*A*). These results are consistent with the assumption that the C-terminal part of Gα_s can move near the WT or D100A protomer, when BIMU8 activates both protomers (Fig. 10*B*).

Positioning the FRET donor on the D100A (instead of WT) protomer confirmed these results. Indeed, upon 5-HT binding to the WT protomer, the labeled N terminus of Gα_s moved
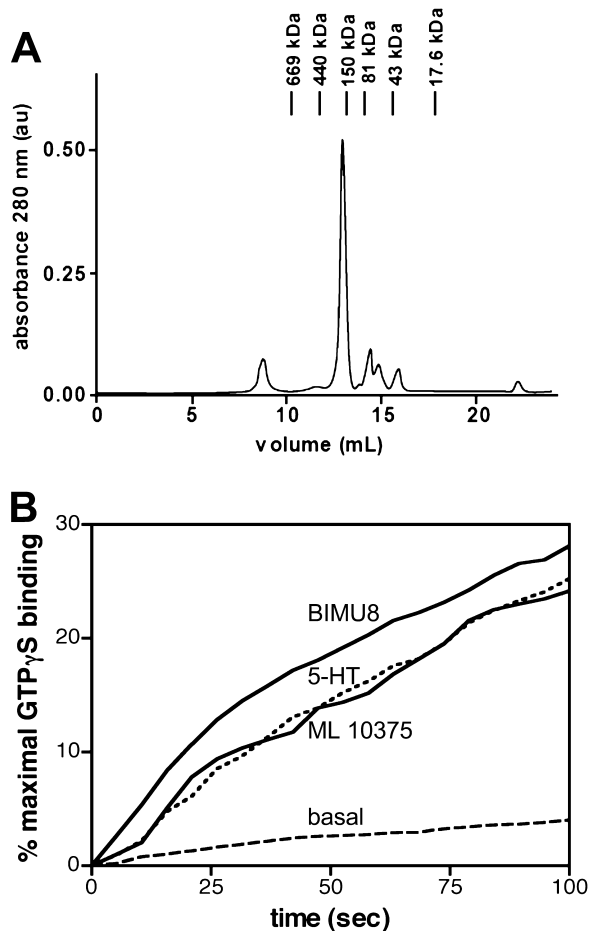
A

B

FIGURE 9. **Activation of G_s protein by purified, recombinant 5-HT$_4$R *in vitro*.** *A*, 5-HT$_4$R·G-protein complex formation assessed by dTSP chemical cross-linking and size exclusion chromatography. Purified 5-HT$_4$R in the presence of 5-HT was cross-linked in the presence of $G\alpha_s\beta_1\gamma_2$ and analyzed by size exclusion chromatography. *B*, WT·D100A 5-HT$_4$R heterodimer-catalyzed BODIPY-FL GTPγS binding to G_s protein. GTPγS binding exchange on $G\alpha_s$ was catalyzed by 10^{-5} M BIMU8, 5-HT, or ML 10375. Data are expressed as a percentage of maximal binding, which was similar whatever the ligand used.

close to the D100A protomer, which resulted in a clear FRET signal (Fig. 10, *C* and *D*). Conversely, upon challenge with ML 10375, which activates only D100A, the N terminus of $G\alpha_s$ moved away from D100A, and, thus, the FRET signal was lowered (Fig. 10, *C* and *D*). BIMU8 induced an intermediate FRET signal, like when WT was used as FRET donor (Fig. 10*A*). Collectively, these experiments confirm the asymmetric positioning of $G\alpha_s$ proteins upon activation of 5-HT$_4$R dimers, with the C terminus being located near the ligand-occupied protomer.

DISCUSSION

Recent data indicate that some class A GPCRs, such as rhodopsin, as well as the β_2-adrenergic, μ-opioid, and neurotensin receptors can activate G proteins as monomers, at least in small lipid vesicles (20, 21, 45, 46). Furthermore, monomeric rhodopsin in solution has been shown to activate transducin at the diffusion limit (47). This clearly indicates that class A GPCRs do not need to dimerize to transduce signals. However, this conclusion should not mask many other data indicating that dimer (and presumably oligomer) formation occurs in class A GPCRs (7).

Dimerization has been mostly studied in terms of assembly and intracellular trafficking. Much less is known about the consequences of dimerization on receptor signaling efficiency. Here, we have addressed this question by using 5-HT$_4$R as a class A GPCR model and by taking advantage of a large variety of mutants, which bind or do not bind to agonists, couple or do not couple to G protein, and can be studied in cellular contexts as well as *in vitro* (34, 35, 40, 41).

Using FRET and saturation binding experiments, we show that 5-HT$_4$Rs behave as dimers or oligomers. We then provide evidence consistent with a model in which complete activation of G signaling by 5-HT$_4$R dimers requires the activation of both protomers. Moreover, our data argue against independent interaction of each protomer of a dimer with a G protein to induce its activation: 1) a dimer, in which both protomers (D66N·D100A) bind to BIMU8 but one (D66N) is unable to couple to G protein, was as active as the (D100A·D100A) dimer composed of two protomers that were both capable of binding to BIMU8 and of interacting with the G protein; 2) purified 5-HT$_4$R dimers associated with an unique heterotrimeric G protein in detergent and formed a pentameric complex, as already proposed for some class A and class C GPCRs (28, 48, 49). Further supporting this pentameric organization, we also demonstrated that the heterotrimeric G protein bound asymmetrically to 5-HT$_4$R homodimers or heterodimers, as shown previously for the BLT1 and mGlu1 receptors (18, 36).

Allosteric interactions between protomers of dimeric GPCRs and their consequences for G protein activation seem to be pleiotropic. Negative cooperativity, which has been reported for chemokine receptor heterodimers (50) and for glycoprotein hormone receptors (12), is consistent with an activation mechanism in which a single ligand molecule binds to a receptor dimer (at least at low concentration). Javitch and co-workers (22) recently reported maximal activation of the dopamine D2 receptor fused to a Gqi5 chimera upon agonist binding to a single protomer. Arcemisbéhère *et al.* (51) found that purified BLT2 receptor monomers in solution activated G_{i2} proteins (GTPγS binding) more efficiently than a solution of dimers at the same receptor concentration. In metabotropic glutamate receptors (mGluRs) (18) as well as in BLT1 receptors (36), only one heptahelical domain is turned on upon activation of these homodimeric receptors when both binding sites are occupied. Conversely, occupation of both protomers is required for full G protein activation by mGluRs (26). Similarly, binding of two ligand molecules is mandatory for 5-HT$_{2C}$ receptor function (27). Furthermore, each subunit of the yeast α-factor receptor is activated independently by agonists, and the subunits cooperate in activating G proteins (52). Other experiments suggest that interaction of M3 muscarinic receptor dimers with β-Arrestin-1 and the subsequent activation of ERK1/2 require binding of an agonist to each receptor protomer (53). In agreement with these last reports, our study demonstrates that the binding of two agonists to 5-HT$_4$R dimers is required to provide full G protein activation.

How two 5-HT$_4$R protomers cooperate to almost double the level of G protein activation in comparison with when a single protomer is activated is unknown. Induction of two subunits leads to a higher GTPγS incorporation rate than following
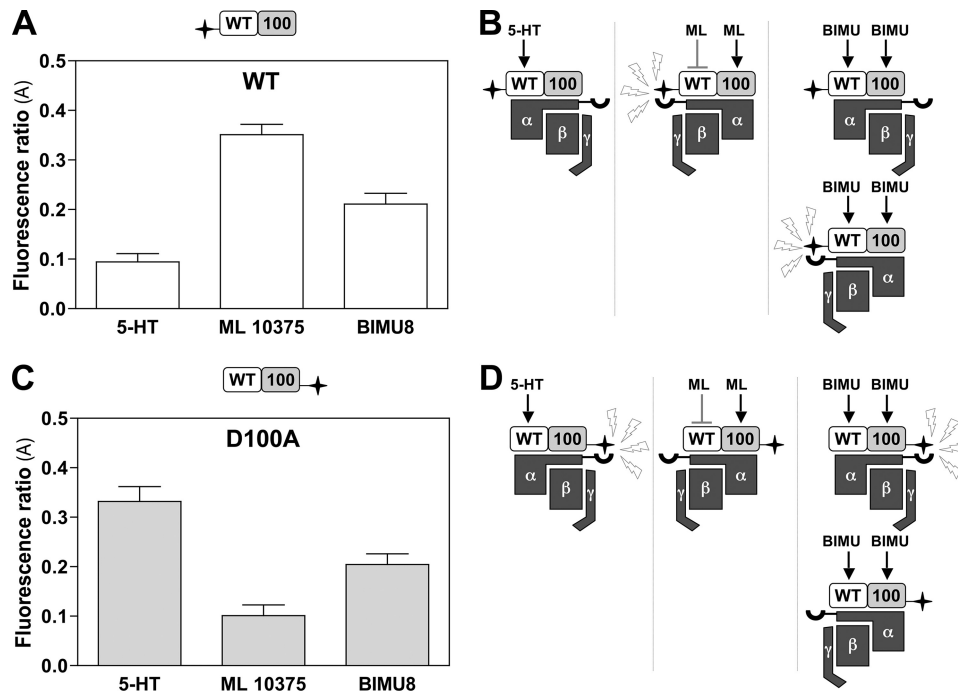
FIGURE 10. **The C terminus of Gα_s binds to the agonist-occupied protomer in WT·D100A purified dimers.** *A* and *C*, FRET signal ratios obtained between WT (*A*) or D100A (*C*) protomers (FRET donors) and Gα_s that was N-terminally labeled with the FRET acceptor, in the presence of 5-HT, ML 10375, or BIMU8 (10^{-5} M). *B* and *D*, schematic representation of the different conformations of dimer·G protein complexes upon 5-HT, ML 10375 (*ML*), or BIMU8 (*BIMU*) activation. *Star*, FRET donor; *half-ring*, FRET acceptor. Fluorescence transfer is represented using *flash symbols. Error bars*, S.E.

activation of a single subunit. Further work is without any doubt necessary to determine how 5-HT$_4$R dimers enhance the GDP/GTP exchange rate. The partial conformational change induced by the activated protomer in the unresponsive protomer observed in biophysical experiments might reflect cross-reactions between both protomers. Thus, when one protomer is occupied by the agonist, the other one adopts a conformation that is different from that of a naive protomer. The hypothesis that binding of a ligand to one protomer might induce a structural change in the other protomer is in agreement with structural data obtained for the chemokine receptor CXCR4 (14). Accordingly, two liganded protomers might form an asymmetric structure when they are occupied by the same agonist (see model in supplemental Fig. 6). Because GPCRs contact both Gα and G$\beta\gamma$ subunits (43), we propose that one 5-HT$_4$R protomer might contact Gα and the other one might contact G$\beta\gamma$, as already suggested by Johnston and Siderovski (44). This is consistent with the observations made on family A and C GPCRs (19, 48) and with the present findings, which show asymmetric binding of the G protein to a dimer.

The mono-, di-, or oligomeric structure of rhodopsin molecules is still a matter of debate. As rhodopsin forms dimers, one can easily understand that the possibility to obtain a response upon occupancy of a single protomer is physiologically relevant (54). Despite a high similarity in their secondary structure, GPCRs respond to a wide range of agonists (from photons to proteins) present at very different concentrations (from one photon in twilight vision to millimolar concentrations of neurotransmitters in synapses) via pleiotropic molecular mechanisms. In this context, the possibility to generate a graduated response, depending on the occupation of one or two binding sites in a GPCR dimer, is an adaptive advantage. This might be

especially relevant in the brain, where GPCRs are often localized at the periphery of synapses (*e.g.* group I mGluRs (55)), far from presynaptic releasing sites (*e.g.* 5-HT receptors (56)).

REFERENCES

1. Bourne, H. R. (1997) *Curr. Opin. Cell Biol.* **9,** 134–142
2. Bockaert, J., and Pin, J. P. (1999) *EMBO J.* **18,** 1723–1729
3. Kobilka, B. K. (2007) *Biochim. Biophys. Acta* **1768,** 794–807
4. Milligan, G. (2001) *J. Cell Sci.* **114,** 1265–1271
5. Bulenger, S., Marullo, S., and Bouvier, M. (2005) *Trends Pharmacol. Sci.* **26,** 131–137
6. Guo, W., Urizar, E., Kralikova, M., Mobarec, J. C., Shi, L., Filizola, M., and Javitch, J. A. (2008) *EMBO J.* **27,** 2293–2304
7. Gurevich, V. V., and Gurevich, E. V. (2008) *Trends Neurosci.* **31,** 74–81
8. Lohse, M. J. (2010) *Curr. Opin. Pharmacol.* **10,** 53–58
9. Chidiac, P., Green, M. A., Pawagi, A. B., and Wells, J. W. (1997) *Biochemistry* **36,** 7361–7379
10. Waldhoer, M., Fong, J., Jones, R. M., Lunzer, M. M., Sharma, S. K., Kostenis, E., Portoghese, P. S., and Whistler, J. L. (2005) *Proc. Natl. Acad. Sci. U.S.A.* **102,** 9050–9055
11. Décaillot, F. M., Rozenfeld, R., Gupta, A., and Devi, L. A. (2008) *Proc. Natl. Acad. Sci. U.S.A.* **105,** 16045–16050
12. Urizar, E., Montanelli, L., Loy, T., Bonomi, M., Swillens, S., Gales, C., Bouvier, M., Smits, G., Vassart, G., and Costagliola, S. (2005) *EMBO J.* **24,** 1954–1964
13. Albizu, L., Cottet, M., Kralikova, M., Stoev, S., Seyer, R., Brabet, I., Roux, T., Bazin, H., Bourrier, E., Lamarque, L., Breton, C., Rives, M. L., Newman, A., Javitch, J., Trinquet, E., Manning, M., Pin, J. P., Mouillac, B., and Durroux, T. (2010) *Nat. Chem. Biol.* **6,** 587–594
14. Wu, B., Chien, E. Y., Mol, C. D., Fenalti, G., Liu, W., Katritch, V., Abagyan, R., Brooun, A., Wells, P., Bi, F. C., Hamel, D. J., Kuhn, P., Handel, T. M.,

Cherezov, V., and Stevens, R. C. (2010) *Science* **330,** 1066–1071

15. Xu, H., Staszewski, L., Tang, H., Adler, E., Zoller, M., and Li, X. (2004) *Proc. Natl. Acad. Sci. U.S.A.* **101,** 14258–14263

16. Filipek, S., Krzysko, K. A., Fotiadis, D., Liang, Y., Saperstein, D. A., Engel, A., and Palczewski, K. (2004) *Photochem. Photobiol. Sci.* **3,** 628–638

17. Park, P. S., Lodowski, D. T., and Palczewski, K. (2008) *Annu. Rev. Pharmacol. Toxicol.* **48,** 107–141

18. Hlavackova, V., Goudet, C., Kniazeff, J., Zikova, A., Maurel, D., Vol, C., Trojanova, J., Prézeau, L., Pin, J. P., and Blahos, J. (2005) *EMBO J.* **24,** 499–509

19. Damian, M., Martin, A., Mesnier, D., Pin, J. P., and Banères, J. L. (2006) *EMBO J.* **25,** 5693–5702

20. Whorton, M. R., Bokoch, M. P., Rasmussen, S. G., Huang, B., Zare, R. N., Kobilka, B., and Sunahara, R. K. (2007) *Proc. Natl. Acad. Sci. U.S.A.* **104,** 7682–7687

21. Whorton, M. R., Jastrzebska, B., Park, P. S., Fotiadis, D., Engel, A., Palczewski, K., and Sunahara, R. K. (2008) *J. Biol. Chem.* **283,** 4387–4394

22. Han, Y., Moreira, I. S., Urizar, E., Weinstein, H., and Javitch, J. A. (2009) *Nat. Chem. Biol.* **5,** 688–695

23. Goudet, C., Kniazeff, J., Hlavackova, V., Malhaire, F., Maurel, D., Acher, F., Blahos, J., Prézeau, L., and Pin, J. P. (2005) *J. Biol. Chem.* **280,** 24380–24385

24. Guo, W., Shi, L., and Javitch, J. A. (2003) *J. Biol. Chem.* **278,** 4385–4388

25. Vilardaga, J. P., Nikolaev, V. O., Lorenz, K., Ferrandon, S., Zhuang, Z., and Lohse, M. J. (2008) *Nat. Chem. Biol.* **4,** 126–131

26. Kniazeff, J., Bessis, A. S., Maurel, D., Ansanay, H., Prézeau, L., and Pin, J. P. (2004) *Nat. Struct. Mol. Biol.* **11,** 706–713

27. Herrick-Davis, K., Grinde, E., Harrigan, T. J., and Mazurkiewicz, J. E. (2005) *J. Biol. Chem.* **280,** 40144–40151

28. Banères, J. L., and Parello, J. (2003) *J. Mol. Biol.* **329,** 815–829

29. Barthet, G., Gaven, F., Framery, B., Shinjo, K., Nakamura, T., Claeysen, S., Bockaert, J., and Dumuis, A. (2005) *J. Biol. Chem.* **280,** 27924–27934

30. Adamus, G., Arendt, A., and Hargrave, P. A. (1991) *J. Neuroimmunol.* **34,** 89–97

31. Claeysen, S., Sebben, M., Becamel, C., Bockaert, J., and Dumuis, A. (1999) *Mol. Pharmacol.* **55,** 910–920

32. Maurel, D., Kniazeff, J., Mathis, G., Trinquet, E., Pin, J. P., and Ansanay, H. (2004) *Anal. Biochem.* **329,** 253–262

33. Barthet, G., Framery, B., Gaven, F., Pellissier, L., Reiter, E., Claeysen, S., Bockaert, J., and Dumuis, A. (2007) *Mol. Biol. Cell* **18,** 1979–1991

34. Claeysen, S., Joubert, L., Sebben, M., Bockaert, J., and Dumuis, A. (2003) *J. Biol. Chem.* **278,** 699–702

35. Banères, J. L., Mesnier, D., Martin, A., Joubert, L., Dumuis, A., and Bockaert, J. (2005) *J. Biol. Chem.* **280,** 20253–20260

36. Damian, M., Mary, S., Martin, A., Pin, J. P., and Banères, J. L. (2008) *J. Biol. Chem.* **283,** 21084–21092

37. McEwen, D. P., Gee, K. R., Kang, H. C., and Neubig, R. R. (2001) *Anal. Biochem.* **291,** 109–117

38. Gether, U., Lin, S., Ghanouni, P., Ballesteros, J. A., Weinstein, H., and Kobilka, B. K. (1997) *EMBO J.* **16,** 6737–6747

39. Conklin, B. R., Hsiao, E. C., Claeysen, S., Dumuis, A., Srinivasan, S., Forsayeth, J. R., Guettier, J. M., Chang, W. C., Pei, Y., McCarthy, K. D., Nissenson, R. A., Wess, J., Bockaert, J., and Roth, B. L. (2008) *Nat. Methods* **5,** 673–678

40. Chang, W. C., Ng, J. K., Nguyen, T., Pellissier, L., Claeysen, S., Hsiao, E. C., and Conklin, B. R. (2007) *PLoS ONE* **2,** e1317

41. Pellissier, L. P., Sallander, J., Campillo, M., Gaven, F., Queffeulou, E., Pillot, M., Dumuis, A., Claeysen, S., Bockaert, J., and Pardo, L. (2009) *Mol. Pharmacol.* **75,** 982–990

42. Berthouze, M., Ayoub, M., Russo, O., Rivail, L., Sicsic, S., Fischmeister, R., Berque-Bestel, I., Jockers, R., and Lezoualc'h, F. (2005) *FEBS Lett.* **579,** 2973–2980

43. Hamm, H. E. (2001) *Proc. Natl. Acad. Sci. U.S.A.* **98,** 4819–4821

44. Johnston, C. A., and Siderovski, D. P. (2007) *Mol. Pharmacol.* **72,** 219–230

45. White, J. F., Grodnitzky, J., Louis, J. M., Trinh, L. B., Shiloach, J., Gutierrez, J., Northup, J. K., and Grisshammer, R. (2007) *Proc. Natl. Acad. Sci. U.S.A.* **104,** 12199–12204

46. Kuszak, A. J., Pitchiaya, S., Anand, J. P., Mosberg, H. I., Walter, N. G., and Sunahara, R. K. (2009) *J. Biol. Chem.* **284,** 26732–26741

47. Ernst, O. P., Gramse, V., Kolbe, M., Hofmann, K. P., and Heck, M. (2007) *Proc. Natl. Acad. Sci. U.S.A.* **104,** 10859–10864

48. Pin, J. P., Kniazeff, J., Liu, J., Binet, V., Goudet, C., Rondard, P., and Prézeau, L. (2005) *FEBS J.* **272,** 2947–2955

49. Jastrzebska, B., Fotiadis, D., Jang, G. F., Stenkamp, R. E., Engel, A., and Palczewski, K. (2006) *J. Biol. Chem.* **281,** 11917–11922

50. Springael, J. Y., Le Minh, P. N., Urizar, E., Costagliola, S., Vassart, G., and Parmentier, M. (2006) *Mol. Pharmacol.* **69,** 1652–1661

51. Arcemisbéhère, L., Sen, T., Boudier, L., Balestre, M. N., Gaibelet, G., Detouillon, E., Orcel, H., Mendre, C., Rahmeh, R., Granier, S., Vivès, C., Fieschi, F., Damian, M., Durroux, T., Banères, J. L., and Mouillac, B. (2010) *J. Biol. Chem.* **285,** 6337–6347

52. Chinault, S. L., Overton, M. C., and Blumer, K. J. (2004) *J. Biol. Chem.* **279,** 16091–16100

53. Novi, F., Stanasila, L., Giorgi, F., Corsini, G. U., Cotecchia, S., and Maggio, R. (2005) *J. Biol. Chem.* **280,** 19768–19776

54. Baylor, D. A., Lamb, T. D., and Yau, K. W. (1979) *J. Physiol.* **288,** 613–634

55. Kuwajima, M., Hall, R. A., Aiba, A., and Smith, Y. (2004) *J. Comp. Neurol.* **474,** 589–602

56. Riad, M., Garcia, S., Watkins, K. C., Jodoin, N., Doucet, E., Langlois, X., el Mestikawy, S., Hamon, M., and Descarries, L. (2000) *J. Comp. Neurol.* **417,** 181–194